Indian Journal of Chemical Technology
Vol. 25, March 2018, pp. 140-149

Porous activated carbon material derived from sustainable bio-resource of peanut shell for H_2 and CO_2 storage applications

Arjunan Ariharan & Balasubramanian Viswanathan*
National Centre for Catalysis Research, Indian Institute of Technology Madras, Chennai 600 036, India
E-mail: bvnathan@iitm.ac.in

Received 18 November 2017; accepted 26 December 2017

Porous activated carbon materials have numerous properties for use in energy storage applications as in adsorbent materials for solid state H_2 and CO_2 storage. In this work, the synthesis of activated porous carbon material derived from the sustainable source of peanut shell (Arachis hypogaea) is described by carbonization and activation processes using KOH as activating agent. The peanut shell derived porous activated carbon material denoted as (PDPAC), shows spherical and sheet like morphology with specific surface area of 1726 m²/g. Interestingly, this peanut derived porous activated carbon material exhibit hydrogen storage capacity of ~1.2 wt% at 298 K and 100 bar pressure. However, the CO_2 storage capacity of 3.5 mmol CO_2 g^{-1} at 298 K and 1.0 bar pressure is achieved. Furthermore, this paper presents the state-of-the-art on the synthesis of activated porous carbon materials with maximization of porosity, the use of cheap biomass waste derived precursors and tailoring of their textural properties.

Keywords: Carbon materials, Activated carbon, Hydrogen storage, Chemical activation, CO_2 storage, Porosity

Of late, renewable (or) sustainable energy and ecological protection are the two important concerns of scientific economy. The general opinion is that hydrogen energy will resolve the difficulty of diminution, effluence and global warming connected with fossil fuels, since hydrogen would be a synthetic fuel because it is lightweight, abundant and its oxidation product (water) is environmentally benign. The lacking relation in hydrogen based energy economy is storage. In order for hydrogen economy should become feasible, certain particular breaking points on hydrogen storage capacity, reversibility and cost viability are the essential conditions which must be fulfilled. However, hydrogen storage is the "bottleneck" that holds up the recognition of DOE on-board purpose of using hydrogen as energy carrier[1-5]. There are numerous ways to store hydrogen, such as liquefaction, compressed gas, metal hydrides, chemical hydrides and in porous adsorbents. Unfortunately, none of these methodologies are good enough to satisfy all the benchmarks like size, efficiency, cost, kinetics and safety compulsory for the transportation applications[6-8]. However, there are other gases that are of interest, such as hydrocarbon for example methane, ecologically essential gases such as CO_2 and SO_2[9]. Each gas and its related applications have criteria that must be met for any gas storage material[10-12]. The improvement of solid state adsorbents that can sequester polluting green-house gases such as CO_2 should be cost-effective and should lead to ecological benefits[13,14]. There is increasing attention on facile and inexpensive synthesis methodologies that bring porous materials with appropriate properties for use as solid state gas adsorbents[15].

Sorption materials like Metal Organic Frameworks (MOF), Covalent Organic Frameworks (COF) and Porous Aromatic Frameworks (PAF), physisorption of gases is preferred due to their kinetic performance, reversibility and relatively high storage capacity. For these issues, carbon materials show good chemical stability, ready availability, high packing density and low cost, all of these make carbon nano-materials more suitable candidate for hydrogen storage.

In view of the above, porous carbon materials including, activated carbon[16], carbon nanotubes[17-19], graphene[20,21], and nano structured carbon materials are being widely explored due to their light weight, fast hydrogen adsorption kinetics and cost effectiveness[16,22,23]. In common, high surface area and micropore volume are important criteria for enhancing the hydrogen storage capacity in carbonaceous materials[24-26]. The selection of materials depends essentially on hydrogen storage to meet the increasing and critical demand for the renewable energy

resources. The cooperation between the high surface area and porous nature in carbon materials imparts enhancement in the hydrogen and CO_2 storage capacity. Now a days, number of procedures have been adopted to synthesize porous carbons, including the template method, physical activation, and the chemical activation[27]. Biomass waste derived activated carbons have become the potential adsorbent materials[28]. These characteristics have widened the usefulness of activated carbons to more demanding applications, such as catalysis/electro catalysis, energy storage in supercapacitors, Li-ion batteries, CO_2 capture and H_2 storage[29].

In recent years, biomass waste products as the carbon sources have been attracting great attention because of their abundance, low cost and sustainability[30]. Biomass wastes are very cheap and easily available, which are potential raw materials for the preparation of porous carbons with good storage performance. The produced carbonaceous materials from bamboo[31], peat moss[32], banana peels[33] and pomelo peels[34] have been shown as the outstanding adsorbent materials for H_2 and CO_2 storage applications. As one of the essential biomass waste products, about 6 million ton of peanut shells have been yearly generated global and the largest part of them have not been entirely utilized but not at least can be applied to produce hierarchical nanostructured carbon materials throughout scalable and inexpensive industrialized processing, a green and sustainable material platform is then achieved to broaden their practical applications for advanced energy storage[35]. Additionally, the pyrolysis of peanut shells derived carbon materials utilized for electrochemical capacitive applications[35-37] has been previously studied, but the hydrogen storage capacity was not investigated in elsewhere.

The chemical activation via a chemical process among carbon and an activated representative is an effective approach for industrially generating micropores and enhancing the specific surface area of carbon materials. While chemical activation involves the impregnation of an activating reagent onto a carbon precursor, which is then heated to high temperature in an oxygen free atmosphere[3,38,39]. The mechanisms for KOH activation of carbon materials can be summarized as follows: First, the carbon matrix is etched by the K-containing species (KOH) through a redox reaction, resulting in abundant micro/mesopores; second step, the water vapour produced in the activation method contributes to the gasification of carbon, which further helps to extend the porosity; Finally, the intermediate products (metallic K) can intercalate into the carbon structure and expand the carbon lattices, leading to a highly porous structure[40,41]. The point of this work is to augment the renewable and sustainable approach in the direction of porous activated carbon material with prominence on the utilization of facile cost-effective and biomass-based precursors.

By this route, one can without difficulty obtain porous carbon material from inexpensive and sustainable Peanut (Arachis hypogaea) shell. The synthesis of activated porous carbon material form most abundant biomass source in world namely, Peanut is available all over the world is described. To the best of our knowledge no report is available, where peanut shell derived carbon material utilized as a H_2 and CO_2 storage applications.

Experimental Section

Materials

Potassium hydroxide (KOH) was purchased from Sigma-Aldrich. Peanut (common name) (Binomial name: Arachis hypogaea, Family: Fabaceae) were collected from Thiruppandurai village Thanjavur district (Tamilnadu, India). (it is also known as ground nut and goober worldwide).

Physical characterization

Wide angle Powder XRD pattern of the calcined carbon materials was recorded using a Rigaku Miniflex II diffractometer with Cu Kα as the radiation source at a wavelength of 0.154 nm with 2θ angle ranging from 10° to 80° with a 0.02 step size. Raman spectroscopy and measurements were performed using HORIBA Lab RAM HR microscope. BET N_2 adsorption and desorption isotherms were measured with surface area and porosity analyzer (Micromeritics Accelerated Surface Area and Porosimetry System (ASAP 2020) for the determination of surface area and total pore volume at 77 K. Before analysis, the samples were oven dried at 150°C and evacuated for 10 h at 200°C under vacuum. The surface area was calculated using the BET method[42]. Based on adsorption data in the partial pressure (P/Po) range 0.02-0.25, and total pore volume was determined from the amount of nitrogen adsorbed at P/Po ca. 0.99 bar. Prior to the adsorption measurements, the sample was degassed at 473K for 6 h. FEI Quanta FEG 200-High Resolution Scanning Electron Microscope (HRSEM) was employed for

obtaining the micrographs. The carbon samples were mounted via conductive carbon double-sided sticky tape. A thin (ca.10 nm) coating of gold sputter was deposited onto the carbon samples to decrease the effects of charging. Jeol JEM-2000 High Resolution Transmission Electron Microscopy (HRTEM) was employed for obtaining the micrographs. The samples for HRTEM were prepared by ultrasonic dispersion of powder carbon samples in ethanol, which was then deposited and dried on a holey carbon film on a copper supported grid. X-ray photoelectron spectroscopy (XPS) measurements were performed with an Omicron Nanotechnology spectrometer with hemispherical analyzer. The monochromatized Mg Kα X-source (E = 1253.6 eV) was operated at 15 *kV* and 20 mA. For the narrow scans, the analyzer pass energy of 25 eV was applied. The base pressure in the analysis chamber is 5×10^{-10} Torr.

Gas adsorption measurements

High pressure volumetric hydrogen adsorption measurements have been carried out using High pressure volumetric analyzer (HPVA-100). The high pressure adsorption analyzer consists of a cylindrical sample cell of known volume (2 cc and 10 cc). The purity of the utilized hydrogen gas (High pure and high pressure 200 bar cylinder) in the hydrogen adsorption experiments is above 99.999%. The HPVA product operating pressure ranges from high vacuum to 100 bar. The span of the sample temperature during analysis can be from cryogenic to 500°C. Sample analysis data collection is fully automated to assure quality data and high reproducibility. All possible care for the possible sources of leak was carefully taken and long blank run tests were carried out. Care has been taken to avoid the errors due to factors such as temperature instability, leaks and additional pressure and temperature effects caused by expanding the hydrogen to the sample cell. The measurements were carried out by utilizing the systematic procedure as follows: Typically the mass of the carbon samples used for hydrogen storage measurements is in the region of 500 mg to 2 g. Earlier to measurement, the samples are degassed and heated at 200°C for approximately 8 h in vacuum. The whole system has been pressurized at the desired value by hydrogen and change in pressure was monitored. All the hydrogen adsorption measurements have been carried out at room temperature. The experiments have been repeated under the same conditions for stability. Furthermore, the CO_2 adsorption measurement also done with the same instrument stated above by using high purity CO_2 cylinder 99.999% for storage purpose. CO_2 uptake isotherms at 298K were obtained over the pressure range of 0-1 bar. This adsorption cycle was repeated several times for the stability.

Synthesis method of porous activated carbon material

Figure 1 shows the schematic illustration of the synthesis methodology of porous carbon material. Typical synthesis procedure is as follows: Good quality dry peanuts are also called as ground nuts were pried open to obtain the shells. The shells were collected and then thoroughly washed with water dried at sunlight and also dried in an oven at 90°C to remove the moisture. For the activation process, the

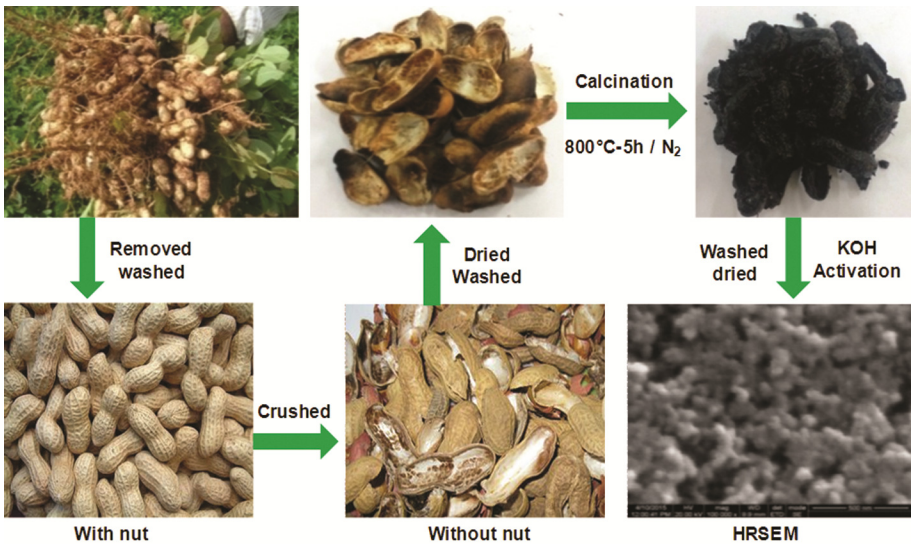

Fig. 1 — Schematic illustration of the peanut shell derived porous activated carbon material

preferred amount of preheated shells was transferred in a quartz boat kept at center of the tubular furnace. The furnace was initially heated at 200°C then continued at 800°C under N_2 atmosphere heating rate employed at 10°C/min. After the calcinations, the tubular furnace automatically cooled to room temperature. The calcined material was washed with distilled water thoroughly. Then, the samples were dried at 90°C overnight to remove moisture. The resulting carbon material was ground into a fine powder using a mortar and pestle. The activation process prepared from carbon material is as follows: The calcined raw peanut derived carbon material was taken as a beaker then added the KOH, in a ratio of 3:1 (KOH 3:1 raw carbon sample), then kept immersed in KOH solution for 24 hr and dried. This mixture was transferred in a quartz boat kept at the tubular furnace, at last the products are carbonized again at 800°C under N_2 atmosphere heating rate employed is at 10°C/min. The calcined material was washed with distilled water thoroughly. Then, the samples were dried at 90°C to remove the moisture. The synthesized activated porous carbon material was then transferred to as scintillation vial for storage, it was utilized to further characterization. The carbon sample without KOH treatment (Peanut Derived Raw Carbon-PDRC) have also been characterized.

Results and Discussion

X-ray diffraction patterns

The X-ray diffraction pattern of the peanut shell derived from porous activated carbon material is shown in Fig. 2 (a). PDPAC shows two broad peaks around 24.0° and 43.4° corresponding to 002 and 100 planes respectively. The peak at around 43.4° (100 plane) is from honeycomb structures formed by sp^2 hybridized carbon framework[41]. For comparison, the PDRC shows same 2-theta value 24.0° but interestingly, after the KOH activation, the defects increased the prepared carbon material because of (43.4°, 100 plane) the increased reflections in intensity. The results suggest an amorphous nature with low crystalline fraction. This is also confirmed by the Raman spectrum of the prepared material as shown in Fig. 2. (b). It is revealed that the porous activated carbon material is likely less crystalline and mostly amorphous in nature.

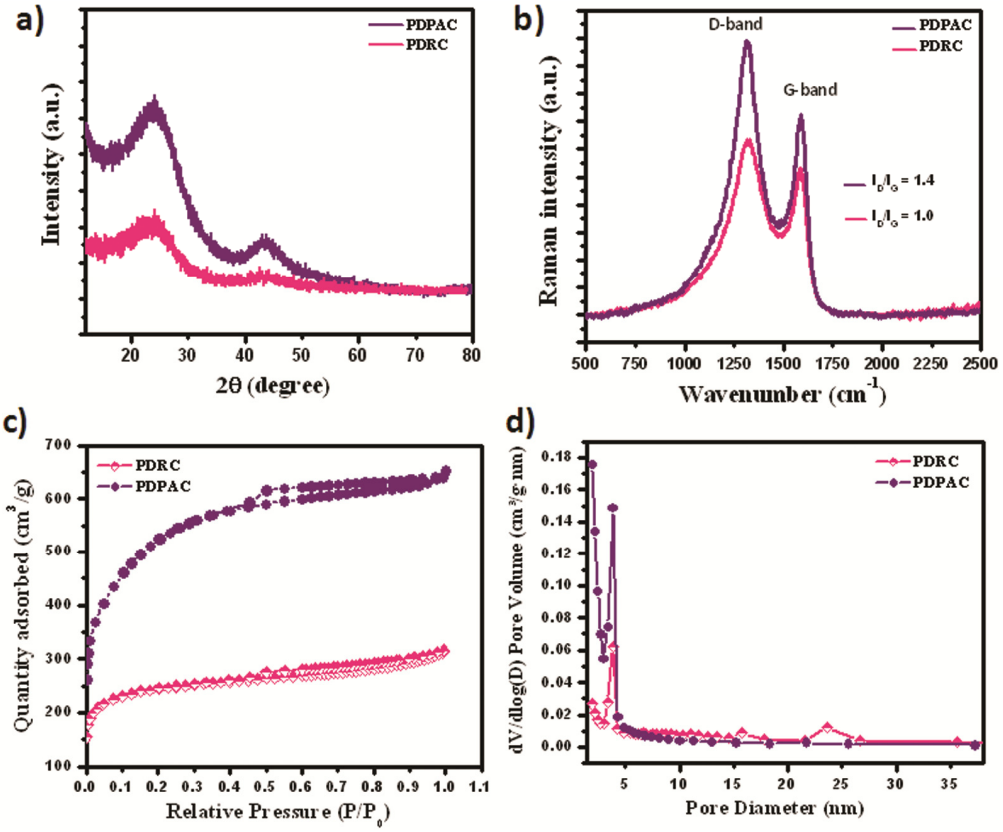

Fig. 2 (a) — X-ray diffraction pattern (b) Raman spectrum (c) BET-N_2 adsorption/desorption isotherm (d) pore size distribution of the peanut shell derived porous activated carbon material

Raman spectroscopy

The Raman spectrum of peanut derived porous activated carbon and raw carbon materials are shown in Fig. 2 (b). The spectrum of PDPAC shows two prominent characteristic peaks located at 1320 and 1585 cm^{-1} which can be assigned to the well-recognized D and G bands of carbon materials. The D band can originate from defects in the structure and disorder-induced features of carbon, while the G band can be ascribed to the vibration of sp^2 hybridized carbon atoms both in chains and rings. Generally, the D/G intensity ratio (I_D/I_G) is commonly accepted as an suitable indicator for the degree of structural disorder of carbon material[43]. However, the intensity ratios of D-band and G-band (I_D/I_G) values is determined to be a slight increase from 1.0 to 1.4 for PDRC and PDPAC respectively, suggesting that the defects and disorder sections in the as-resulted PDPAC is increased with an chemical activation.

BET—N_2 adsorption/desorption isotherms and poresize distribution

In order to further examine, the porosity of the synthesized porous activated carbon material is characterized by BET-N_2 adsorption/desorption isotherm measurements at 77 K. The pore size distribution curves were determined using the Barrett-Joyner-Halenda (BJH) method and are shown in Figs 2 (c) and (d). These isotherms reveal the presence of different pore sizes of micropores and mesopores. However this N_2 sorption showed a type I sorption isotherm with a higher nitrogen sorption capacity below relative pressure (P/Po) = 0.1, which is ascribed to micropore filling signifying the higher ultra-microporous property[44,45]. This suggests that a large proportion of the porosity in the carbons is in the micropore range, which is consistent with the presence of micropore channels arising from the activation process of carbon material[46,47]. Interestingly, a type H4 hysteresis loop has been associated with the existence of slit-shaped micropores positioned between randomly arranged in disordered nature of the synthesized carbon microstructures this is conformity of HRTEM images (Figure. 4). Additionally, the total pore volume of PDPAC increased to 1.08 cm^3/g, while the micropore volume to 0.283 cm^3/g compared to the PDRC sample, the total pore volume was 0.48 cm^3/g and the micropore volume was 0.178 cm^3/g owing to the presence of plentiful micropores because of KOH activation process of the synthesized material. The BET specific surface area values of PDPAC are also higher than that of PDRC and the values are 1726 m^2/g and 810 m^2/g respectively. These data are summarized in Table 1.

HRSEM images

High resolution scanning electron micrographs of the peanut shell derived porous activated carbon material are shown in Fig. 3. The images were taken at different magnifications for the conformation of oriented morphology. The lower magnification Images showed the sheet and inter connected small spherical like morphology. (Figs 3 (a) and (b)). Figures 3 (c) and (d) showed the spheres interconnected with each other one by one it will make the porous nature of the prepared material. The results given above both micropores and mesopores were homogeneously disseminated in the carbon matrix. The morphological modification brought out by KOH activation route demonstrates that a sufficient amount of KOH is essential to form the interconnected cavities within the carbon texture. The assembly of the present microporous carbons is facile and inexpensive and for the moment, they can be engaged as envoy carbonaceous materials for hydrogen storage study in view of the difference of their morphologies and textures.

HRTEM images

The high resolution transmission electron micrographs of the peanut shell derived porous activated carbon material are shown in Fig. 4. HRTEM micrographs show the array one by one of arranged porous sheets like morphology of the prepared material (Fig. 4(a)). Interestingly, the small mesopores are also observed in this prepared materials (Figs 4 (b) and c). However, this morphology is highly favourable for good pore development due to the fact that it provides a large interfacial area for the reaction between the carbon framework and the activation agent (KOH). Furthermore, Figures 4 (d, e and f) showed clearly large

Table 1 — BET-N_2 adsorption/desorption isotherms and poresize distribution data for the synthesized carbon materials.

Sample name	Surface area ($m^{2/g}$)	Extemal surface Area($m^{2/g}$)	Micropore Area ($m^{2/g}$)	Total pore Volume ($cm^{3/g}$)	Micropore volume ($cm^{3/g}$)
PDPAC	1726	1184	530	1.08	0.283
PDRC	810	248	432	0.48	0.178

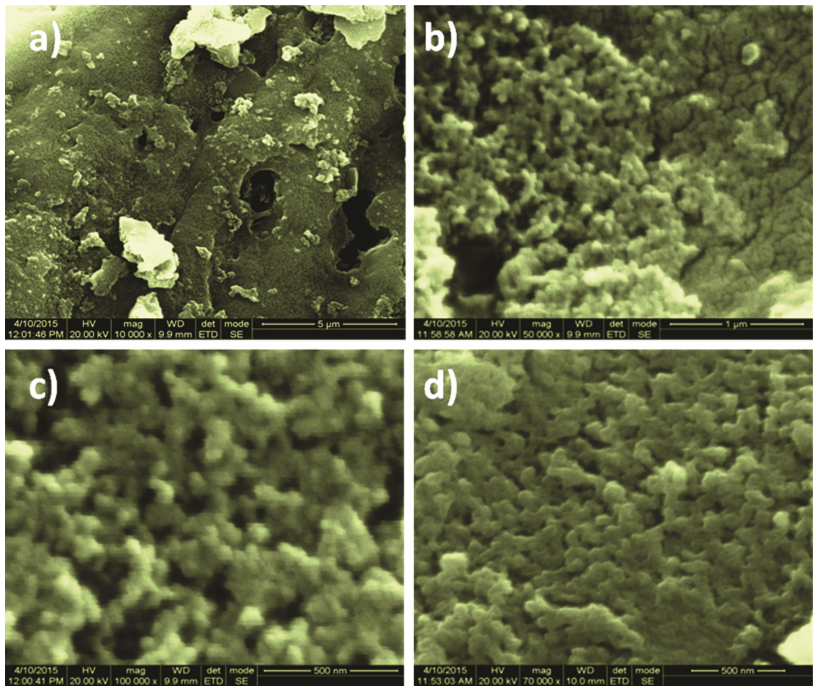

Fig. 3 — High resolution scanning electron microscopy (HRSEM) images of the peanut shell derived porous activated carbon material (Different magnification)

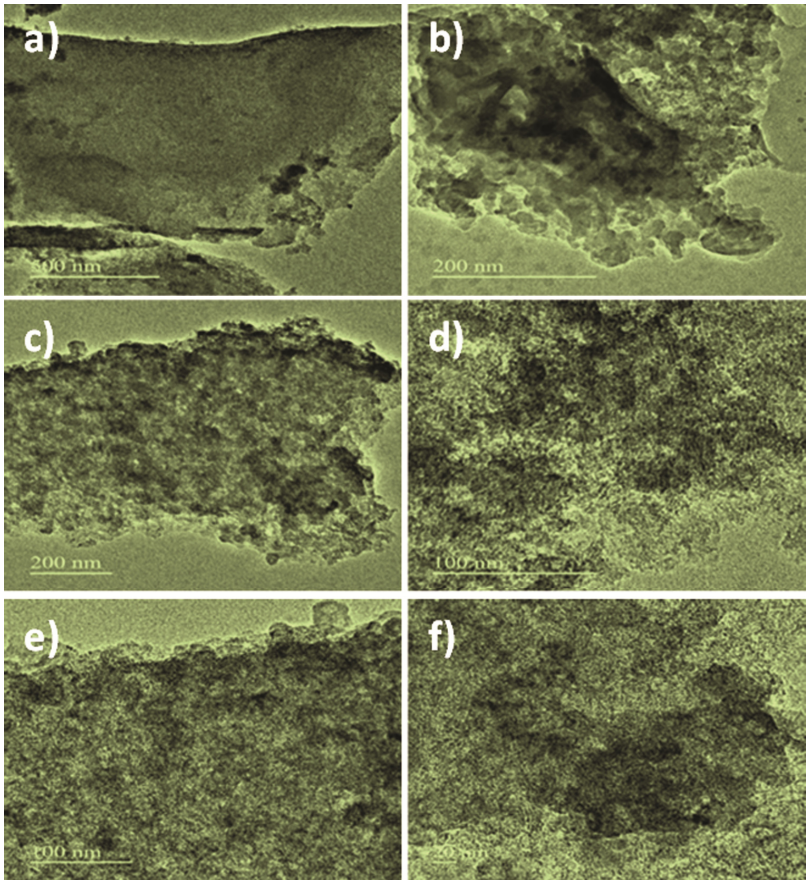

Fig. 4 — High resolution transmission electron microscopy (HRTEM) images of the peanut shell derived porous activated carbon material (Different magnifications)

large number of micropores and also ultramicropores present in this porous carbon material. The HRTEM image of the activated carbon PDPAC evidences that the porosity is made up of randomly oriented uniform micropores. Texture properties of the samples are reliable with morphology characterization; both signifying that the pore structures of biomass-waste derived carbons can be tuned to an extent by adjusting the carbonization and the KOH activation parameters.

X-ray photoelectron spectroscopy

XPS investigation was carried out to establish the precise amount of functional component, detailed surface chemical composition of the peanut shell derived porous activated carbon material and oxygen, the results are shown in Fig. 5. The XPS survey spectrum of the prepared material are shown in Fig. 5 (a). It showed the presence of carbon and oxygen functionality. The C1s peaks at 284.6 eV, 284.8 eV, 284.7 eV, 286.2eV and 288.8 eV (Fig. 5 (b)) are attributed to C–O, sp^3-Carbon and/or sp^2-Carbon, O–C=O and C–OH respectively[47]. In addition, the peak at ~286.2 eV is probably attributed to ester (O–C=O) and carboxyl/carbonyl (C–OH) groups, these high binding energy components may shift the peak to 3-4 eV beyond the main carbon peak. The last peak at 288.8 eV could be described to Plasmon loss features[48]. The high resolution O1s spectra could be deconvoluted into 3 peaks around 530.4 eV, 531.5 and 532.1 (Fig. 5 (c)) representing the 3 different types of oxygen functional groups C–O/O–C=O, and C=O quinone type groups (530.4 eV), also this peak arise due to high binding energy bonds between oxygen and carbon such as the C–O/C–OH bond in ester and carboxyl groups, C–OH phenol/C–O–C ether groups (531.5eV), and COOH carboxylic groups (535.4 eV). The several oxidation led to an raise of oxygen functionalities in the form of ketones and carboxylic groups.

Thermo gravimetric analysis (TGA)

To determine the carbonization temperature, we conducted the thermo-gravimetric analysis of the peanut shell derived porous activated carbon material and is shown in Fig. 5 (d). TGA investigations provide information on the thermal stability of the carbon materials. The first endotherm and weight loss observed around 100-200°C was caused by the loss of

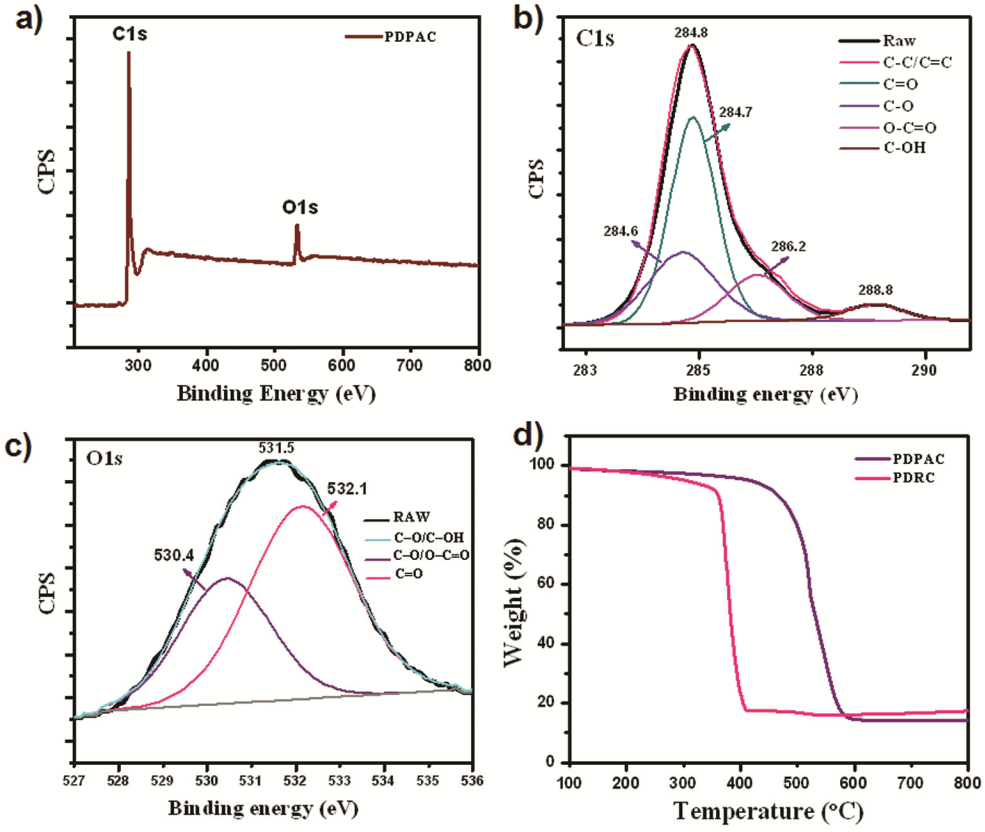

Fig. 5 (a) — XPS survey spectrum (b) C1s (c) O1s and (d) Thermo gravimetric analysis (TGA) profile of the peanut shell derived porous activated carbon material

superficial moisture, volatiles and also removal of physisorbed water from the crushed peanut shell waste[49]. Herein, the pure carbon material shows the TGA curves with increase in temperature, the carbon decomposes rapidly in air with initial decomposition temperature of 400°C and exhausts at 500°C as the final decomposition temperature. This weight loss can be ascribed to combustion of amorphous carbon with small amounts of turbostratic carbon. An additional change that occurs at temperatures higher than 600°C can be attributed to carbon layer formation. The physical processes related with the desorption of moisture from the shells and the chemical processes coupled with the subsequent decomposition reactions are essentially endothermic since the system has to absorb heat from its environment to raise its enthalpy to the critical limit of thermodynamic stability, outside which desorption/decomposition occurs[50]. It was established that KOH confined in the micropores has a better thermal stability under an inert atmosphere compared to KOH confined within the micro/small mesopores. Finally, TGA analysis shows that the precursor of peanut shell which can effortlessly be changed into carbon materials with a high carbon yield, signified that it is a suitable precursor for preparing cost-effective porous carbon materials.

Gas sorption isotherms

The hydrogen adsorption/desorption isotherm of synthesized peanut derived porous activated carbon material is shown in Fig. 6 (a). The hydrogen adsorption isotherm has been carried out at 298 K and 100 bar pressure. Interestingly, no hysteresis is observed in the isotherms, confirming absolutely reversible adsorption and desorption of hydrogen by the prepared porous carbon materials. The peanut derived porous activated carbon (PDPAC) material shows hydrogen storage capacity of ~1.2 wt% at 298 K and 100 bar pressure. The peanut derived raw carbon (PDRC) material showed hydrogen storage capacity of ~0.5 wt% at room temperature and 100 bar, which is less than that observed for the Peanut derived porous activated (PDPAC) carbon material. A relationship between maximum hydrogen adsorption capacity and micropore volume has also been observed for carbons with a wide range of functionalities and porous structures with respect to the KOH activation[26]. These correlations point out the primary significance of porous structural characteristics and secondary significance of surface interactions between hydrogen gas and carbon sorbent. However, the carbon materials with high total pore volumes do not essentially have likewise high hydrogen adsorption capacities. It is obvious that narrow pores, where the adsorption capacity is improved, are essential for adsorption at low pressure range[5,7]. Furthermore, the large pores offer improved the adsorption ability at higher pressure range. Consequently, when preparing the porous carbon structures for hydrogen storage purpose, there is a cooperation which has to be made among adsorption capability and also adsorption at lower pressure range. There are also several proofs that the density of adsorbed hydrogen decreases with rising pore size of the adsorbent material[5,51]. The present carbon samples have a high proportion of microporosity as discussed above, which is beneficial to high performance hydrogen uptake.

The CO_2 adsorption capacities of the peanut derived porous activated carbon materials were

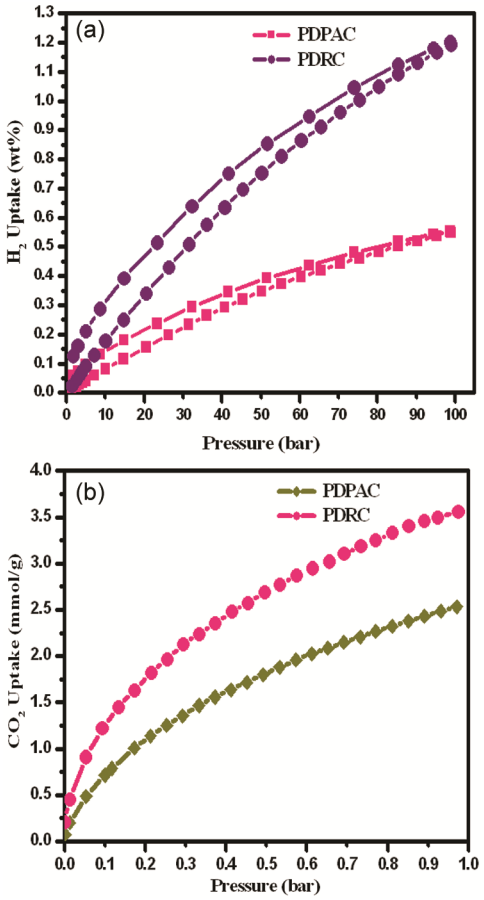

Fig. 6 (a) — H_2 adsorption/desorption isotherm and (b) CO_2 adsorption isotherm of the peanut shell derived porous activated carbon material

investigated at 298 K. A comparative purpose of analysis of the CO_2 adsorption isotherms of the porous activated carbon and unactivated raw carbon samples namely PDPAC and PDRC, it is shown in Fig. 6 (b). It can be seen that the CO_2 capture capacities of the PDRC shows the CO_2 uptake capacity of 2.2 mmol/g at 25°C and 1.0 bar. The CO_2 adsorption capacity of 3.5 mmol/g at 25°C and 1.0 bar for the peanut derived porous activated carbon material (PDPAC) compared to the peanut derived raw carbon material (PDRC). Likewise, this comparative investigation reveals that the KOH activation process significantly enhances the CO_2 adsorption capacity. These overall, results reveal that the storage capacity of the adsorbents not only depends on the textural properties of BET surface area or pore volume but also on the pore size distribution, as we have already pointed out in relation to other activated carbons[52,53]. It is important to bear this in mind when designing CO_2 carbon sorbents. Interestingly, the amount of CO_2 adsorbed depends generally on the population of narrow slit type micropores, which make a significant contribution to CO_2 storage.

Conclusion

The porous activated carbon material is prepared utilizing peanut shell as precursor. This as-prepared porous activated carbon material show hydrogen storage capacity of ~1.2 wt% at 298 K and 100 bar. The CO_2 adsorption capacity of synthesized PDPAC shows 3.5 mmol/g at 298 K and 1.0 bar. This work provides an environmental friendly and trustworthy methodology to prepare valuable porous activated carbon material from renewable biomass waste which shows potential for gas storage application.

Acknowledgement

The authors wish to record their grateful thanks to the Department of Science and Technology (DST), New Delhi, India for supporting the National Centre for Catalysis Research (NCCR), Indian Institute of Technology Madras (IITM), Chennai, India, Ministry New and Renewable Energy (MNRE), Government of India, New Delhi, for supporting the hydrogen storage activity of this centre.

References

1 Wang H, Gao Q & Hu J, *J Amer Chem Soc*, 131 (2009) 7016.
2 Konwar R J & De M, *Int J Hydrogen Energy*, 41 (2016) 21300.
3 Sevilla M, Fuertes A B & Mokaya R, *Energy Environ Sci*, 4 (2011) 1400.
4 Masika E & Mokaya R, *Energy & Environmental Science*, 7 (2014) 427.
5 Thomas K M, *Catal Today*, 120 (2007) 389.
6 Schlapbach L & Züttel A, *Nature*, 414 (2001) 353.
7 Zhao X B, Xiao B, Fletcher A J & Thomas K M, *J Phys Chem B*, 109 (2005) 8880.
8 Ariharan A, Viswanathan B & Nandhakumar V, *Int J Hydrogen Energy*, 41 (2016) 3527.
9 Sevilla M, Sangchoom W, Balahmar N, Fuertes A B & Mokaya R, *ACS Sustain Chem Eng*, 4 (2016) 4710.
10 Morris R E & Wheatley P S, *Angew Chem Int Ed*, 47 (2008) 4966.
11 Robertson C & Mokaya R, *Microporous Mesoporous Mater*, 179 (2013) 151.
12 Sevilla M, Falco C, Titirici M M & Fuertes A B, *RSC Adv*, 2 (2012) 12792.
13 Wang Q, Luo J, Zhong Z & Borgna A, *Energy Environ Sci*, 4 (2011) 42.
14 Sevilla M & Fuertes A B, *J Colloid Interface Sci*, 366 (2012) 147.
15 Van den Berg A W C & Arean C O, *Chem Commun*, (2008) 668.
16 Wang J, Senkovska I, Kaskel S & Liu Q, *Carbon*, 75 (2014) 372.
17 Dillon A C, Jones K M, Bekkedahl T A, Kiang C H, Bethune D S & Heben M J, *Nature*, 386 (1997) 377.
18 Sankaran M, Viswanathan B & Srinivasa Murthy S, *Int J Hydrogen Energy*, 33 (2008) 393.
19 Sankaran M & Viswanathan B, *Carbon*, 45 (2007) 1628.
20 Wang L, Stuckert N R & Yang R T, *AIChE J*, 57 (2011) 2902.
21 Ariharan A, Viswanathan B & Nandhakumar V, *Graphene*, 5 (2016) 39.
22 Liu X, Zhang C, Geng Z & Cai M, *Microporous Mesoporous Mater*, 194 (2014) 60.
23 Züttel A, Sudan P, Mauron P, Kiyobayashi T, Emmenegger C & Schlapbach L, *Int J Hydrogen Energy*, 27 (2002) 203.
24 Yang Z, Xia Y & Mokaya R, *J Amer Chem Soc*, 129 (2007) 1673.
25 Pacula A & Mokaya R, *J Phys Chem C*, 112 (2008) 2764.
26 Jordá-Beneyto M, Suárez-García F, Lozano-Castelló D, Cazorla-Amorós D & Linares-Solano A, *Carbon*, 45 (2007) 293.
27 Lee J, Kim J & Hyeon T, *Adv Mater*, 18 (2006) 2073.
28 Ariharan A, Viswanathan B & Nandhakumar V, *Int J Hydrogen Energy*, 41 (2016) 3527.
29 Tang W, Zhang Y, Zhong Y, Shen T, Wang X, Xia X & Tu J, *Mater Res Bull*, 88 (2017) 234.
30 Arrebola J C, Caballero A, Hernán L, Morales J, Olivares-Marín M & Gómez-Serrano V, *J Electrochem Soc*, 157 (2010) A791.
31 Jiang J, Zhu J, Ai W, Fan Z, Shen X, Zou C, Liu J, Zhang H & Yu T, *Energy Environ Sci*, 7 (2014) 2670.
32 Ding J, Wang H, Li Z, Kohandehghan A, Cui K, Xu Z, Zahiri B, Tan X, Lotfabad E M, Olsen B C & Mitlin D, *ACS Nano*, 7 (2013) 11004.
33 Lotfabad E M, Ding J, Cui K, Kohandehghan A, Kalisvaart W P, Hazelton M & Mitlin D, *ACS Nano*, 8 (2014) 7115.
34 Hong K I, Qie L, Zeng R, Yi Z Q, Zhang W, Wang D, Yin W, Wu C, Fan Q J, Zhang W X & Huang Y H, *J Mater Chem A*, 2 (2014) 12733.

35 Ding J, Wang H, Li Z, Cui K, Karpuzov D, Tan X, Kohandehghan A & Mitlin D, *Energy Environ Sci*, 8 (2015) 941.
36 Lv W, Wen F, Xiang J, Zhao J, Li L, Wang L, Liu Z & Tian Y, *Electrochim Acta*, 176 (2015) 533.
37 Cao X, Chen S & Wang G, *Electron Mater Lett*, 10 (2014) 819.
38 Sevilla M, Fuertes A B & Mokaya R, *Int J Hydrogen Energy*, 36 (2011) 15658.
39 Sevilla M, Mokaya R & Fuertes A B, *Energy Environ Sci*, 4 (2011) 2930.
40 Wang J & Kaskel S, *J Mater Chem*, 22 (2012) 23710.
41 Cao Y, Wang K, Wang X, Gu Z, Fan Q, Gibbons W, Hoefelmeyer J D, Kharel P R & Shrestha M, *Electrochim Acta*, 212 (2016) 839.
42 Brunauer S, Emmett P H & Teller E, *J Amer Chem Soc*, 60 (1938) 309.
43 Choi C, Seo S D, Kim B K & Kim D W, *Sci Rep*, 6 (2016) 39099.
44 Ou J, Zhang Y, Chen L, Zhao Q, Meng Y, Guo Y & Xiao D, *J Mater Chem A*, 3 (2015) 6534.
45 Ghosh S, Sevilla M, Fuertes A B, Andreoli E, Ho J & Barron A R, *J Mater Chem A*, 4 (2016) 14739.
46 Alam N & Mokaya R, *Energy Environ Sci*, 3 (2010) 1773.
47 Cheng F, Liang J, Zhao J, Tao Z & Chen J, *Chem Mater*, 20 (2008) 1889.
48 Kostoglou N, Tarat A, Walters I, Ryzhkov V, Tampaxis C, Charalambopoulou G, Steriotis T, Mitterer C & Rebholz C, *Microporous Mesoporous Mater*, 225 (2016) 482.
49 Rybarczyk M K, Peng H J, Tang C, Lieder M, Zhang Q & Titirici M M, *Green Chem*, 18 (2016) 5169.
50 Fey G T K, Lee D, Lin Y & Kumar T P, *Synth Metals*, 139 (2003) 71.
51 Lin X, Jia J, Zhao X, Thomas K M, Blake A J, Walker G S, Champness N R, Hubberstey P & Schröder M, *Angew ChemInt Ed*, 45 (2006) 7358.
52 Sevilla M, Valle-Vigón P & Fuertes A B, *Adv Funct Mater*, 21 (2011) 2781.
53 Sevilla M & Fuertes A B, *Energy Environ Sci*, 4 (2011) 1765.